Quantum network of atom clocks: a possible implementation with neutral atoms

P. Kómár,[1] T. Topcu,[1,2,3] E. M. Kessler,[1,3] A. Derevianko,[1,2,3] V. Vuletić,[4] J. Ye,[5] and M. D. Lukin[1]

[1]*Physics Department, Harvard University, Cambridge, MA 02138, USA*
[2]*Department of Physics, University of Nevada, Reno, NV 89557, USA*
[3]*ITAMP, Harvard-Smithsonian Center for Astrophysics, Cambridge, MA 02138, USA*
[4]*Department of Physics and Research Laboratory of Electronics, Massachusetts Institute of Technology, Cambridge, MA 02139, USA*
[5]*JILA, NIST, Department of Physics, University of Colorado, Boulder, CO 80309, USA*

(Dated: May 21, 2016)

We propose a protocol for creating a fully entangled GHZ-type state of neutral atoms in spatially separated optical atomic clocks. In our scheme, local operations make use of the strong dipole-dipole interaction between Rydberg excitations, which give rise to fast and reliable quantum operations involving all atoms in the ensemble. The necessary entanglement between distant ensembles is mediated by single-photon quantum channels and collectively enhanced light-matter couplings. These techniques can be used to create the recently proposed quantum clock network based on neutral atom optical clocks. We specifically analyze a possible realization of this scheme using neutral Yb ensembles.

PACS numbers: 03.67.Ac, 03.67.Bg 32.80.Rm

The current record in clock accuracy is held by ytterbium and strontium clocks [1], capable of reaching $\sim 10^{-18}$ fractional frequency stability [2, 3]. Apart from the enormous amount of effort and innovation, the unprecedented precision and accuracy were attainable due to the large number of clock atoms ($10^3 - 10^4$) [4]. Superstable clocks enable evaluation of the systematic frequency shift of atomic transitions with less avergaging time, which is important to measure fast transients, e.g. gravitational waves and passing dark-matter clumps [5]. In our recent work [6], we showed that a quantum network of atomic clocks can result in substantial boost of the overall precision if multiple clocks are connected in quantum entanglement. The proposed globally entangled state, Greenberger-Horne-Zeilinger (GHZ) state, is more sensitive to the global phase evolution of the clock atoms, thus allows for an improved measurement of the passage of time. If the GHZ state is set up and interrogated in the optimal way [7, 8], frequency measurements can asymptotically reach the Heisenberg limit [9], associated with the total number of atoms in the entire network. Significant noise reduction has recently been demonstrated with spin-squeezed states in a single ensemble of atoms [10]. Efforts are being made to make both the non-local [11] and local entanglement distribution [12, 13] faster and more reliable. Of particular interest are applications of these ideas to neutral atom clocks.

In this Letter, we show how a non-local GHZ state can be created across multiple, spatially separated neutral atom clocks with high fidelity. Our protocol relies on strong Rydberg blockade for enhancing local atom-atom interaction, collective excitations for enhancing photon-atom interaction, and single photon quantum channels for reliable remote connections. We propose and analyze a realization using neutral Yb ensembles, suitable for the current atomic clock technology. We predict that thousands of atoms can be entangled to give an overall stability increase of more than an order of magnitude, compared to non-entangled clock networks. We emphasize that our protocol, although presented to be used for a network, can also be applied to a single ensemble.

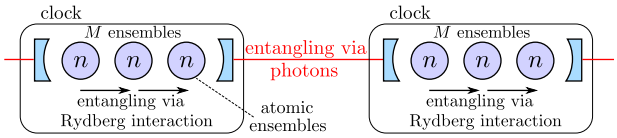

FIG. 1. (Color online) Schematic of the setup. K clocks, each holding M atomic ensembles of size n are connected. Atoms within each ensemble get entangled using long-range interaction between Rydberg atoms, ensembles in the same clock are entangled either via Rydberg interactions or via the cavity mode, while neighboring clocks are entangled through single-photon quantum channels, enhanced by optical cavities. The resulting state is a global GHZ state, $|0\rangle^{\otimes N} + |1\rangle^{\otimes N}$ of all $N = KMn$ atoms in the network.

We describe our protocol for K identical atomic clocks arranged in a sequence, each connected to its neighbors with optical channels, and each using Mn identical atoms, trapped in a magic-wavelength optical lattice, distributed in M ensembles, illustrated on Fig. 1. We use the atomic levels, shown on Fig. 2(a) for our protocol: The two levels of the clock transition, g, f, a metastable shelving level s, an excited level e, which spontaneously decays to g, and two strongly interacting Rydberg levels, r_1 and r_2. We further require transitions between levels, marked with arrows, to be driven independently.

We imagine preparing all atoms in the ground state g, after which our protocol consists of five subsequent steps. First, using blockade, we create two independent collective excitations in one ensemble in each clock, using two separate atomic levels (f and s). Second, each excited

ensemble emits single photon pulses that are entangled with one of these collective excitations. Third, the photons are sent towards the neighboring atomic clocks, and measured with a linear optics setup in Bell-basis. Fourth, upon success, each clock performs a local CNOT operation to connect the two collective excitations. The result is a set of K entangled collective excitations, one in the first ensemble of each clock, which serve as "seeds" for a global GHZ state. In the fifth, and final, step the clocks locally "grow" a GHZ state out of each seed, extending it to all atoms in the clock, and thus a global GHZ state is obtained. In the following, we provide detailed description and analysis of these five steps, discuss the specific realization in Yb atoms and analyze the most important sources of imperfections and errors.

Our scheme makes use of the Rydberg blockade, which is a result of the interaction arising between atoms excited to Rydberg states in an ensemble. If driven resonantly, the first excited atom blocks the transition of a second one, thus at most one atom can get coherently excited to the Rydberg state [14–16], allowing precise quantum control. Rydberg blockade has been proposed as an efficient tool to realize quantum gates and perform quantum information processing [13, 17–21]. Efficient control requires the atoms to reside within the blockade radius of the Rydberg atom. Different ways of trapping and manipulating Rydberg states are currently under investigation both experimentally [22–26] and theoretically [27–29].

In the first step, we make use of the Rydberg blockade to create a superposition of one and zero excitation in both f and s levels, following the approach of [13, 14, 17]. This is done by performing the following sequence of driving pulses: $[\pi/(2\sqrt{n})]_{g,r1}$, $[\pi]_{f,r1}$, $[\pi]_{f,s}$, $[(\pi/(2\sqrt{n})]_{g,r1}$, $[\pi]_{f,r1}$, shown in Fig. 2(a), where $[\phi]_{a,b}$ stands for a pulse with total, single-atom Rabi phase ϕ between level a and b. Starting from the state $|g\rangle^{\otimes n} =: |0_f 0_s\rangle$, this pulse sequence creates the state

$$(1+f^\dagger)(1+s^\dagger)|0_f 0_s\rangle =: \Big(|0_f\rangle + |1_f\rangle\Big)\Big(|0_s\rangle + |1_s\rangle\Big), \quad (1)$$

where $f^\dagger$ and $s^\dagger$ are creation operators of the two (approximately) independent spin wave modes, supported by the two levels f and s. The kets, $|n_f\rangle, |n_s\rangle$ for $n \in \{0, 1\}$ stand for collective spin waves being excited by n quanta.

In the second step, spin-photon entangled states, using the spin wave modes f and s, are created, based on an extended version of the scheme described in [30] and collective enhancement. Each spin-photon entangled state is created by the pulse sequence shown in Fig. 2(b), involving $[\pi]_{s,r2}$, $[\pi/\sqrt{n}]_{g,r1}$, $[\pi]_{e,r1}$, $[\pi]_{s,r2}$. This particular sequence results in emitting a single photon (from $e \to g$ transition) provided that the level s is empty: $|0_s\rangle|\text{vacuum}\rangle \to |0_s\rangle|1 \text{ photon}\rangle$. With additional pulses applied before and after this sequence flipping between

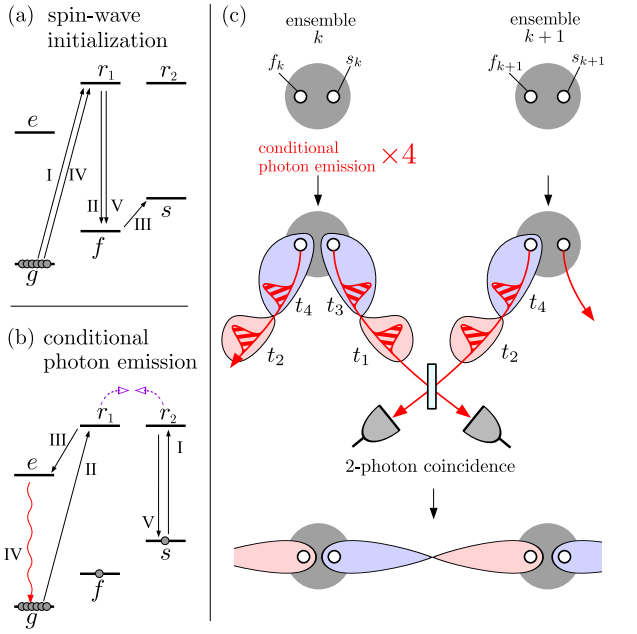

FIG. 2. (Color online) Steps to generate pairwise entanglement. (a) Pulse sequence used to initialize the spin-waves f and s in an ensemble. (b) Pulse sequence inducing a conditional photon emission, the emitted photon becomes entangled with the spin state s. (c) In three steps, neighboring ensembles generate pairwise entanglement between their collective excitations. First, they induce $0+1$ superpositions of the two independent spin waves, $f^\dagger$ and $s^\dagger$. Then applying the conditional photon emission sequence four times, they emit four pulses, containing two photons total. Each pair of photons is correlated with a unique spin state. Finally, photons are measured with a linear optics setup, and 2-photon coincidences indicate the creation of entanglement between neighboring ensembles. (Blue and red shadings indicate positive and negative correlation between qubits, respectively.)

$0_f \leftrightarrow 1_f$, $0_s \leftrightarrow 1_s$ and swapping f and s waves, and proper timing, this is repeated four times to produce four time-bin separated light pulses, which are entangled with the two spin waves,

$$\Big(|0_f\rangle|t_2\rangle + |1_f\rangle|t_4\rangle\Big)\Big(|0_s\rangle|t_1\rangle + |1_s\rangle|t_3\rangle\Big), \quad (2)$$

where $|t_j\rangle|t_k\rangle$ is a two photon state with photons emitted at times t_j and t_k.

In the third step, pairs of time-bin encoded photon pulses from two neighboring ensembles are detected by interfering the two pulses on a beam splitter and measuring two-photon coincidences [31–33]. As a result, entangled states between neighboring atomic ensembles, k and $k+1$, are created [34, 35],

$$|0_s\rangle_k|1_f\rangle_{k+1} \pm |1_s\rangle_k|0_f\rangle_{k+1}, \quad (3)$$

where the individual kets represent the states of f and s spin waves in the two ensembles, see Fig. 2(c).

In the fourth step, the ensembles perform a local CNOT operation on the two collective degrees of free-

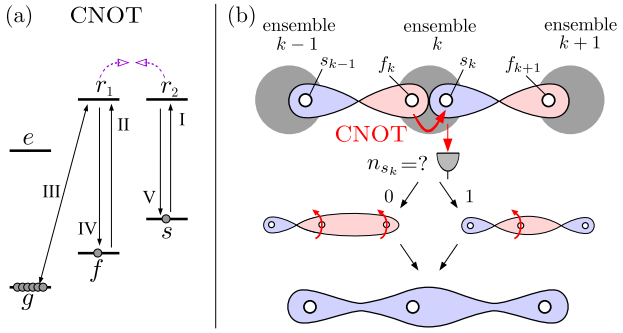

FIG. 3. (Color online) Connecting links into non-local GHZ state. (a) CNOT gate between the two excitations f and s: If level s is occupied, then the coherent (de)excitation of the f level is blocked by the Rydberg blockade between the r_1 and r_2 intermediate levels, otherwise it succeeds. (b) Connecting two entanglement links. The local CNOT and measurement operations on ensemble k entangle the two, initially independent, parts of the system: s_{k-1}, f_k and s_k, f_{k+1}. Depending on the outcome of the measurement, either only f_k, or the entire right hand side needs to be flipped, in order to arrive to the proper GHZ state.

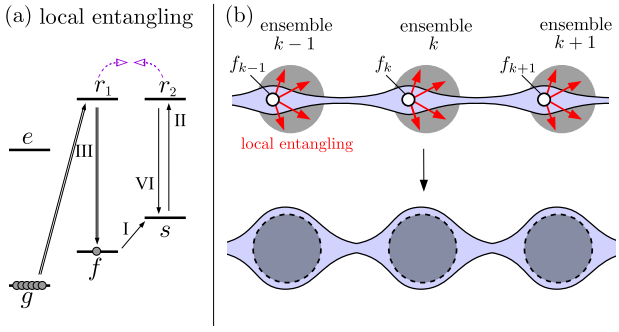

FIG. 4. (Color online) Local GHZ creation. (a) Conditional, local GHZ state generation: Any excitation in level s prevents the transfer from g to f. (b) The local entangling operation extends the GHZ state from the f spin-wave to all atoms. As a result, every atom in the network gets entangled.

dom, $f^\dagger$ and $s^\dagger$. This is done with the following pulse sequence, $[\pi]_{s,r2}$, $[\pi]_{f,r1}$, $[\pi/\sqrt{n}]_{g,r1}$, $[\pi]_{f,r1}$, $[\pi]_{s,r2}$, shown on Fig. 3(a). This promotes any population in s to r_2, which then blocks the path $g \leftrightarrow r_1 \leftrightarrow f$. The result is a conditional flip $|0_f\rangle \leftrightarrow |1_f\rangle$, conditioned on having zero $s^\dagger$ excitations. If we perform $f \leftrightarrow s$ swaps before and after this process, we get a coherent flip between $|0_f, 0_s\rangle \leftrightarrow |0_f, 1_s\rangle$.

To understand the resulting state, let us consider two entangled links, connecting three neighboring ensembles $k-1, k$ and $k+1$ as shown in Fig. 3(b). The corresponding state, before the fourth step, is

$$\left(|0_{s_{k-1}}, 1_{f_k}\rangle + |1_{s_{k-1}}, 0_{f_k}\rangle\right) \otimes \left(|0_{s_k}, 1_{f_{k+1}}\rangle + |1_{s_k}, 0_{f_{k+1}}\rangle\right), \quad (4)$$

where $|n_{s_{k-1}}, n_{f_k}\rangle \otimes |n_{s_k}, n_{f_{k+1}}\rangle$ indicate the number of excitations in the modes $s_{k-1}, f_k, s_k, f_{k+1}$ of the three ensembles. After the conditional flip of s_k and measurement of n_{s_k}, yielding $m \in \{0, 1\}$, the state becomes $|0, 1, 1-m\rangle + |1, 0, m\rangle$, where the remaining kets stand for $|n_{s_{k-1}}, n_{f_k}, n_{f_{k+1}}\rangle$. Depending on the outcome, either only f_k (if $n_{s_k} = 1$) or the entire right hand side (if $n_{s_k} = 0$) needs to be flipped in order to obtain the desired GHZ state, $\bigotimes_k |0_{f_k}\rangle + \bigotimes_k |1_{f_k}\rangle$, of the f excitations of each clock, $k = 1, 2, \ldots K$.

In the fifth step, each clock locally extends the entanglement from its f degree of freedom to all atoms using a collective Rydberg gate similar to the ones introduced in Refs. [36, 37]. In the case when each clock consists of a single blockaded ensemble, the pulse sequence $[\pi]_{f,s}$, $[\pi/2]_{s,r2}$, $\left([\pi/\sqrt{n-j+1}]_{g,r1}, [\pi/\sqrt{j}]_{f,r1}\right.$ for $\left.j = 1, 2, \ldots n\right)$, $[\pi]_{s,r2}$, shown in Fig. 4(a), does exactly that. This sequence transfers the atoms one by one from g to f only if r_2 is unoccupied, and gets blocked otherwise. The result is

$$\bigotimes_{k=1}^{K} |0_f\rangle_k + \bigotimes_{k=1}^{K} |1_f\rangle_k \rightarrow \bigotimes_{k=1}^{K} |f\rangle^{\otimes n} + \bigotimes_{k=1}^{K} s^\dagger |g\rangle^{\otimes n}, \quad (5)$$

where $|f\rangle$ and $|g\rangle$ denote the state of a single atom. Finally, we get rid of the s excitation with a series of pulses that move it back to g: $[\pi]_{f,s}$, $[\pi]_{f,r1}$, $[\pi]_{f,s}$, $[\pi/\sqrt{n}]_{g,r1}$, and end up with $|f\rangle^{\otimes Kn} + |g\rangle^{\otimes Kn}$, a fully entangled state of all $N = Kn$ atoms in the network.

In practice, lattice clocks can employ $n = 10^3 - 10^4$ atoms each, that can not be manipulated simultaneously with high fidelity using Rydberg blockade (see discussion below). In such a case, the atoms can be separated into $M \sim 10$ ensembles within each clock, as shown in Figure 1. Efficient local entanglement can be achieved with techniques described in [38] or by using an individually addressed "messenger" atom, that can be moved to the vicinity of each ensemble to entangle all atoms within each clock using dipole-dipole interaction. In such a case, the messenger atom can used, first, to extend the entanglement to all ensembles in each clock, resulting in a state $|1_f\rangle^{KM} + |0\rangle^{KM}$, after which the procedure shown in Fig. 4(a) applied within each ensemble can be used to a fully entangled state of all $N = K \times Mn$ atoms in the network. (See Supplementary for details.)

Next, we investigate the robustness of our protocol in light of realistic physical imperfections. We assume that all imperfections decrease the coherence between the two components of the GHZ state, and therefore the fidelity can be written as $F = [1 + \exp(-\varepsilon_{\rm tot})]/2$, where $\varepsilon_{\rm tot}$ is the sum of the errors. The errors arising during each non-local connection step $\varepsilon_{\text{non-local}}$ and the errors arising during a local GHZ creation in one clock $\varepsilon_{\rm local}$ add up to the total error

$$\varepsilon_{\rm tot} = (K-1)\varepsilon_{\text{non-local}} + KM\varepsilon_{\rm local}. \quad (6)$$

This error increases linearly with the total number

of atoms in the network, N, and the coefficient, $(\varepsilon_{\text{non-local}}/M + \varepsilon_{\text{local}})/n$, depends on the number of atoms, n, within a single atom cloud under blockade. For a certain optimal local atom number n_{opt}, the total fidelity is maximal, i.e. decreases with the slowest rate, as N increases.

To be specific, we focus on a possible implementation of our scheme with ensembles of neutral ytterbium atoms whose relevant electronic levels are shown on Fig. 5. We identify the following levels of neutral Yb relevant

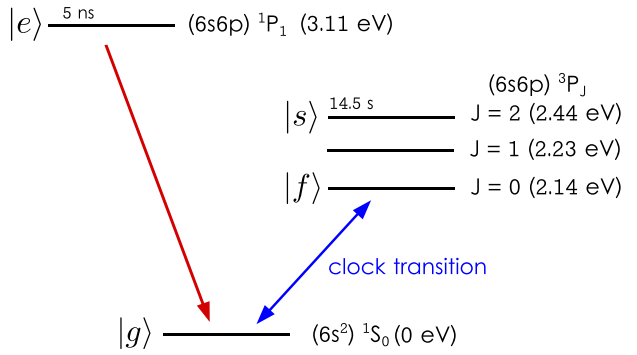

FIG. 5. (Color online) Implementation of our protocol in the lower level of neutral Yb. We assign the roles of g and f to the clock levels, the role of s to the metastable $J = 2$ level of $6s6p$, and the role of e to the $^1P_1$ excited state, which spontaneously decays to the ground state.

for our protocol: $|g\rangle = |6s^2(^1S_0)\rangle$, $|f\rangle = |6s6p(^3P_0)\rangle$, $|s\rangle = |6s6p(^3P_2)\rangle$ and $|e\rangle = |6s6p(^1P_1)\rangle$, and two Rydberg levels $|r_1\rangle = |6s\tilde{n}p_{m=+1}(^1P_1)\rangle$ and $|r_2\rangle = |6s\tilde{n}s(^3S_1)\rangle$ with the same principle quantum number $\tilde{n}$. Collective enhancement and phase matching of the laser pulses make the emitted photons leave in a well-defined, narrow solid angle, resulting in high photon collection efficiency. Due to the different symmetries of these states, the coherent coupling can be done via 1-photon transitions for $r_1 \leftrightarrow g$ and $r_2 \leftrightarrow s$, and requires 2-photon transitions for $r_1 \leftrightarrow e$ and $r_1 \leftrightarrow f$. We envision the atoms being held in position by an optical lattice with period $a = 275.75$ nm, each potential minimum holding exactly one Yb atom. (The lattice intensity can be modulated during the Rydberg state excitation [39].) Overall fidelity turns out to depend on the lattice geometry; it is the highest for 3D optical lattice.

We consider the following errors in our analysis. During non-local connection, we take into account the finite r_1-r_2 interaction, which allows the creation of an r_1 excitation with some small probability, even if r_2 is populated, the finite lifetime of the s and r_2 levels, and the dark-count rate of photo-detectors. For the local GHZ creation step, we account for the same imperfection of the r_1-r_2 blockade as for the non-local entangling step, the finite lifetimes of the Rydberg levels r_1 and r_2, and the imperfect self-blockade of the single excited Rydberg states r_1. (See Supplementary Materials for details.) We

Errors in 3D ensemble	error per atom	ratio in total
imperfect blockade (e_1)	2.6×10^{-6}	14%
Rydberg decay (e_2)	1.6×10^{-5}	86%
self-blockade (e_3)	$\sim 10^{-11}$	$< 0.1\%$
r_2 decay (non-local) (e_4)	$\sim 10^{-11}$	$< 0.1\%$
photon detection (e_5)	$\sim 10^{-12}$	$< 0.1\%$
memory error (e_6)	$\sim 10^{-8}$	$< 0.1\%$
photon collection (e_7)	$\sim 10^{-8}$	$< 0.1\%$
total error per atom	1.8×10^{-5}	100%

TABLE I. The absolute and relative contribution of the different error sources to the total error per atom E, at $\tilde{n} = 120$, $\Omega = \Omega_{\text{opt}} = 10^5\,\gamma$ and $n = n_{\text{opt}} = 146$, after numerical optimization, for a 3D lattice. (See Supplementary Materials for 2D results.)

estimate the effect of these errors, and numerically optimize the free parameters: the Rabi frequency Ω of the transferring pulses $g \to r_1$ and $r_1 \to f$, and the number of local atoms n, for principle quantum numbers, $50 \le \tilde{n} \le 150$ of the Rydberg levels, in order to find the minimal error per atom, $E := \varepsilon_{\text{tot}}/N$.

To illustrate, for Rydberg levels $\tilde{n} = 120$, we find that the highest fidelity is reached for $n_{\text{opt}} \approx 146$, and $\Omega = 10^5\,\gamma$, where $\gamma \sim 10^3\,\text{s}^{-1}$ is the natural linewidth of the Rydberg levels, for a clock size of $(Mn)_{\text{opt}} = 2500$. In this case, the error per atom is $E_{\min} = [\varepsilon_{\text{tot}}/N]_{\min} = 1.8 \times 10^{-5}$. Contributions of the different error sources are shown in Table I. We find that the decay of the Rydberg level, and imperfect blockade cause the majority of imperfections, both arising during the critical step, local extension of the GHZ state. (See Supplementary Materials for more details.)

With the optimal ensemble size n_{opt}, determined above, we consider the total number of entangled atoms N. Although having more atoms always results in improved clock precision, entangling all available atoms is not necessarily optimal. To see this, we compare the stability of the entangled clock network and a non-entangled network, and find an optimal entangled atom number N_{opt} by maximizing the stability gain over the non-entangled scheme,

$$G = \frac{\sigma_{\text{non-ent}}}{\sigma_{\text{ent}}/(2F-1)} = e^{-EN}\frac{\pi}{8}\sqrt{\frac{N}{\log N}}, \qquad (7)$$

where $\sigma_{\text{ent}} = \frac{1}{\omega_0\tau}\frac{8}{\pi}\frac{\sqrt{\log N}}{N}$ (from [6], assuming perfect fidelity, and that τ is smaller than the reduced atomic coherence time $\gamma_{\text{at}}^{-1}/N$) and $\sigma_{\text{non-ent}} = \frac{1}{\omega_0\tau}\frac{1}{\sqrt{N}}$ (for N independent atoms) are the Allan deviations of the two schemes, where ω_0 is the central frequency and τ is the total available measurement time. The additional factor of $2F - 1 = e^{-EN}$ is due to the reduced Fisher information of a non-pure GHZ state, where F is the fidelity of the initial state. (See supplementary materials for details.) For $E = E_{\min} = 1.8 \times 10^{-5}$, Eq. (7) is maximized with optimal atom number $N_{\text{opt}} \approx 1/(2E_{\min}) \approx 25000$,

where $G_{\max} \sim 12$, and $F = [1 + e^{-N_{\rm opt}E_{\min}}]/2 = 0.82$. The optimal gain is achieved by 25000 entangled atoms distributed in $K_{\rm opt} = N_{\rm opt}/(Mn)_{\rm opt} \approx 10$ clocks.

We presented and analyzed a protocol, capable of fully entangling ensembles of neutral atoms located in different atomic clocks. Local interactions are made robust by utilizing the strong interaction between Rydberg excitations, and non-local entanglement creation is made reliable with strong atom-light coupling, suppressed photon propagation errors and long atomic memory lifetimes. We showed that our scheme, in particular a realization with neutral Yb ensembles, is feasible and provides significant gain over non-entangled schemes even in the light of physical imperfections. Our results provide the first detailed proposal for a neutral atom clock network that can serve as a first prototype of the global quantum clock network outlined in [6].

We are grateful to Kyle Beloy, Shimon Kolkowitz, Ronen Kroeze, Travis Nicholson, Thibault Peyronel, Alp Sipahigil, Jeff Thompson, and Leo Zhou for enlightening discussions. This work was supported by NSF, CUA, NIST, NASA, Simons Foundation, AFOSR MURI, ARL and NSSEFF fellowship.

[1] A. D. Ludlow and J. Ye, Comptes Rendus Physique **16**, 499 (2015).
[2] N. Hinkley, J. A. Sherman, N. B. Phillips, M. Schioppo, N. D. Lemke, K. Beloy, M. Pizzocaro, C. W. Oates, and A. D. Ludlow, Science **341**, 1215 (2013).
[3] B. J. Bloom, T. L. Nicholson, J. R. Williams, S. L. Campbell, M. Bishof, X. Zhang, W. Zhang, S. L. Bromley, and J. Ye, Nature **506**, 71 (2014).
[4] T. Nicholson, S. Campbell, R. Hutson, G. Marti, B. Bloom, R. McNally, W. Zhang, M. Barrett, M. Safronova, G. Strouse, W. Tew, and J. Ye, Nature Communications **6**, 6896 (2015).
[5] A. Derevianko and M. Pospelov, Nature Physics **10**, 933 (2014).
[6] P. Kómár, E. M. Kessler, M. Bishof, L. Jiang, A. S. Sørensen, J. Ye, and M. D. Lukin, Nature Physics **10**, 582 (2014).
[7] E. M. Kessler, P. Kómár, M. Bishof, L. Jiang, A. S. Sørensen, J. Ye, and M. D. Lukin, Phys. Rev. Lett. **112**, 190403 (2014).
[8] D. W. Berry, B. L. Higgins, S. D. Bartlett, M. W. Mitchell, G. J. Pryde, and H. M. Wiseman, Phys. Rev. A **80**, 052114 (2009).
[9] M. J. W. Hall, D. W. Berry, M. Zwierz, and H. M. Wiseman, Phys. Rev. A **85**, 041802 (2012).
[10] O. Hosten, N. J. Engelsen, R. Krishnakumar, and M. A. Kasevich, Nature **529**, 505 (2016).
[11] N. Sangouard, C. Simon, H. de Riedmatten, and N. Gisin, Rev. Mod. Phys. **83**, 33 (2011).
[12] A. Sørensen and K. Mølmer, Phys. Rev. Lett. **82**, 1971 (1999).
[13] M. Saffman, T. G. Walker, and K. Mølmer, Rev. Mod. Phys. **82**, 2313 (2010).
[14] Y. O. Dudin and A. Kuzmich, Science **336**, 887 (2012).
[15] Y. O. Dudin, A. G. Radnaev, R. Zhao, J. Z. Blumoff, T. A. B. Kennedy, and A. Kuzmich, Phys. Rev. Lett. **105**, 260502 (2010).
[16] M. Ebert, M. Kwon, T. G. Walker, and M. Saffman, Phys. Rev. Lett. **115**, 093601 (2015).
[17] M. D. Lukin, M. Fleischhauer, R. Cote, L. M. Duan, D. Jaksch, J. I. Cirac, and P. Zoller, Phys. Rev. Lett. **87**, 037901 (2001).
[18] M. Müller, I. Lesanovsky, H. Weimer, H. P. Büchler, and P. Zoller, Phys. Rev. Lett. **102**, 170502 (2009).
[19] B. Zhao, M. Müller, K. Hammerer, and P. Zoller, Phys. Rev. A **81**, 052329 (2010).
[20] Y. Han, B. He, K. Heshami, C.-Z. Li, and C. Simon, Phys. Rev. A **81**, 052311 (2010).
[21] M. H. Goerz, E. J. Halperin, J. M. Aytac, C. P. Koch, and K. B. Whaley, Phys. Rev. A **90**, 032329 (2014).
[22] Y.-A. Chen, X.-H. Bao, Z.-S. Yuan, S. Chen, B. Zhao, and J.-W. Pan, Phys. Rev. Lett. **104**, 043601 (2010).
[23] F. Bariani, Y. O. Dudin, T. A. B. Kennedy, and A. Kuzmich, Phys. Rev. Lett. **108**, 030501 (2012).
[24] O. Firstenberg, T. Peyronel, Q.-Y. Liang, A. V. Gorshkov, M. D. Lukin, and V. Vuletić, Nature **502**, 71 (2013).
[25] M. Antezza, C. Braggio, G. Carugno, A. Noto, R. Passante, L. Rizzuto, G. Ruoso, and S. Spagnolo, Phys. Rev. Lett. **113**, 023601 (2014).
[26] T. M. Weber, M. Höning, T. Niederprüm, T. Manthey, O. Thomas, V. Guarrera, M. Fleischhauer, G. Barontini, and H. Ott, Nature Physics **11**, 157 (2015).
[27] T. Topcu and A. Derevianko, Phys. Rev. A **88**, 043407 (2013).
[28] I. I. Beterov, M. Saffman, E. A. Yakshina, V. P. Zhukov, D. B. Tretyakov, V. M. Entin, I. I. Ryabtsev, C. W. Mansell, C. MacCormick, S. Bergamini, and M. P. Fedoruk, Phys. Rev. A **88**, 010303 (2013).
[29] T. Topcu and A. Derevianko, Phys. Rev. A **89**, 023411 (2014).
[30] L. Li, Y. O. Dudin, and A. Kuzmich, Nature **498**, 466 (2013).
[31] L. M. Duan, M. D. Lukin, J. I. Cirac, and P. Zoller, Nature **414**, 413 (2001).
[32] T. Honjo, H. Takesue, H. Kamada, Y. Nishida, O. Tadanaga, M. Asobe, and K. Inoue, Optics Express **15**, 13957 (2007).
[33] A. Rubenok, J. A. Slater, P. Chan, I. Lucio-Martinez, and W. Tittel, Phys. Rev. Lett. **111**, 130501 (2013).
[34] M. Lukin, Rev. Mod. Phys. **75**, 457 (2003).
[35] D. Shwa, R. D. Cohen, A. Retzker, and N. Katz, Phys. Rev. A **88**, 063844 (2013).
[36] M. Saffman and K. Mølmer, Phys. Rev. Lett. **102**, 240502 (2009).
[37] H. Weimer, M. Müller, I. Lesanovsky, P. Zoller, and H. P. Büchler, Nature Physics **6**, 382 (2010).
[38] A. Sørensen, L.-M. Duan, J. I. Cirac, and P. Zoller, Nature **409**, 63 (2000).
[39] T. G. Tiecke, J. D. Thompson, N. P. de Leon, L. R. Liu, V. Vuletič, and M. D. Lukin, Nature **508**, 241 (2014).